Journal of Communications Technology and Electronics, Vol. 45, No. 2, 2000, pp. 179–185. Translated from Radiotekhnika i Elektronika, Vol. 45, No. 2, 2000, pp. 196–203.

DYNAMIC CHAOS IN RADIOPHYSICS AND ELECTRONICS

Chaotic Synchronization in a Network of Symmetrically Coupled Oscillators

V. S. Anishchenko, V. V. Astakhov, V. V. Nikolaev, and A. V. Shabunin

Received October 17, 1997

Abstract—Self-synchronization in a network of two symmetrically coupled chaotic oscillators differing in time scale is studied. The oscillators have a piecewise linear nonlinearity and are coupled via a resistor. For two chaotic oscillations, a definition of the degree of synchronism is suggested on the basis of the coherence function averaged over frequencies. On–off intermittence, which arises with synchronism breaking, is considered. The regions of robust and nonrobust synchronism are delineated.

INTRODUCTION

The synchronization of chaotic oscillations attracts the attention of many researchers. As is known, chaotic synchronism may be complete or incomplete. By complete synchronism, we understand that the oscillations are identical [$\vec{x}_1(t) = \vec{x}_2(t)$] [1, 2] or, in a wider sense, that there exists a functional relation between them [$\vec{x}_1(t) = \vec{f}(\vec{x}_2(t))$] [3]. (In the latter case, the term generalized synchronization is used.) The types of incomplete synchronization reported are the acquisition of the frequencies corresponding to spikes in the oscillation spectra [4] and the acquisition of the instantaneous phases of the analytic signals constructed from oscillations by means of the Hilbert transform [5]. Where incomplete synchronization is concerned, including its upgrading to complete synchronization, the definition of the degree of synchronism becomes an issue.

Recent studies attach much importance to the robustness of chaotic synchronism. Without this property, the synchronism attained by coupled identical oscillators may be destroyed if the identity is broken by an infinitesimal mismatch between the oscillator parameters or if noise is added, at however low a level [6–8]. A violation of synchronism may show up in a number of ways. On–off intermittence [9] is one of them. Viewed from the standpoint of fluid turbulence, the phenomenon manifests itself in turbulent bursts that occasionally interrupt laminar flow. During the bursts, the representative point strays from the symmetric subspace $x_1 = x_2$ so that the x_1, x_2 projection of the phase portrait of the chaotic attractor becomes smeared. The behavior is called the bubbling of the attractor [6].

This study addresses the transition from asynchronous to synchronized chaos. We consider a network of two oscillators that have a piecewise linear nonlinearity and are symmetrically coupled via a resistor, the oscillators being Chua's circuits. It will be demonstrated that, depending on the coupling factor, the network operates in one of the following regimes: asynchronous chaos, incompletely synchronous chaos, nonrobust synchronous chaos, and robust synchronous chaos. In order to evaluate the degree of synchronism between chaotic oscillations, we propose to use an integral quantity based on the averaged cross-spectral density (the coherence function) of the oscillations. On–off intermittence is observed in the region of nonrobust synchronous chaos if a mismatch between the oscillators is brought in, the rate of bursts rising with the mismatch ratio.

DESCRIPTION OF THE NETWORK

Figure 1 shows the network of two symmetrically coupled Chua's circuits and the piecewise linear *V–I*

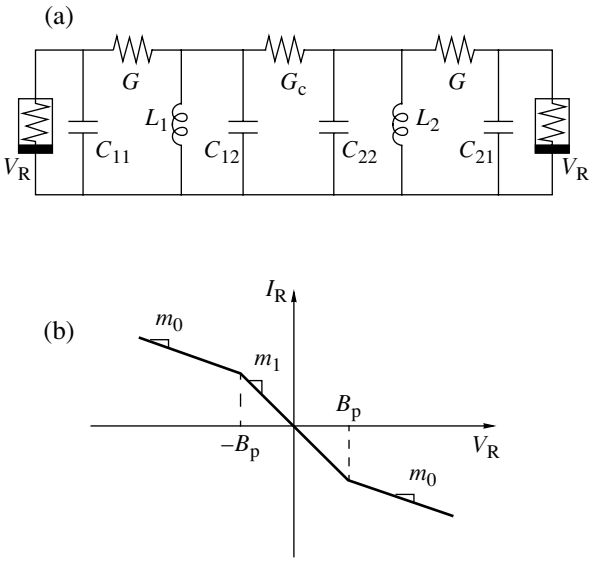

Fig. 1. (a) Network of coupled Chua's circuits and (b) the *V–I* curve of the nonlinear components.

curve of the nonlinear components. Using Kirchhoff's laws and the normalization from [10], we obtain a system of differential equations for the network:

$$\begin{aligned}
\dot{x}_1 &= \alpha(y_1 - x_1 - f(x_1)),\\
\dot{y}_1 &= x_1 - y_1 + z_1 + \gamma(y_2 - y_1),\\
\dot{z}_1 &= -\beta y_1,\\
\dot{x}_2 &= p[\alpha(y_2 - x_2 - f(x_2))],\\
\dot{y}_2 &= p[x_2 - y_2 + z_2 + \gamma(y_1 - y_2)],\\
\dot{z}_2 &= p[-\beta y_2].
\end{aligned} \tag{1}$$

In the context of this study, the circuits have identical nonlinear components and equal conductances, and the reactive components meet the constraint

$$\frac{C_{12}}{C_{22}} = \frac{C_{11}}{C_{21}} = \frac{L_1}{L_2} = p.$$

Consequently, the circuits differ only in time scale: with zero coupling, oscillations in circuit 1 proceed p times slower than those in circuit 2 [4].

We performed numerical experiments with the system at

$$\alpha = 11.9, \quad \beta = 22, \quad a = -\frac{8}{7}, \text{ and } b = -\frac{5}{7},$$

coupling factor γ and mismatch ratio p being chosen for external adjustment.

An uncoupled Chua's circuit is a self-excited oscillator with 1.5 degrees of freedom and three equilibrium points. It exhibits a transition to chaos via a cascade of period-doubling bifurcations. As a result of the chaotic evolution, the attractors created around different equilibrium points merge into the double scroll [11].

Coupled Chua's circuits behave in a more complex fashion. The network may undergo various types of bifurcation: period doubling, the creation and breakdown of a 2-torus, symmetry breaking, and the merging of symmetric limit sets [10]. It essentially possesses multistability, i.e., the property that a number of attractors coexist. This stems from the fact that each cycle involved in a cascade of period doublings undergoes bifurcation twice: being stable, the cycle bifurcates with respect to a first multiplier; then it bifurcates with respect to the other multiplier, acquiring the saddle type. The process ends in groups of limit cycles with equal periods and different time shifts between the oscillations in the respective circuits: two period-2 cycles, four period-4 cycles, eight period-8 cycles, etc. The time shifts turn out to be multiples of the period of the 1-revolution cycle with which the cascade began. Some of the saddle-type cycles thus created become stable at certain parameter values. The rules are also obeyed by other coupled systems with period doubling [12]: *RL*–diode circuits, logistic maps [13], Chua's circuits with capacitive coupling [14], etc.

RESULTS OF NUMERICAL EXPERIMENTS

Chaotic synchronization was studied with the network adjusted for a band chaotic attractor (Figs. 2a, 2b). The experiments were based on system (1). If the oscillators are adjusted identically so that $p = 1$, then increasing γ makes the network go successively through asynchronous chaos (Fig. 2c), incompletely synchronous chaos (Figs. 2d, 2e), and synchronous chaos (Fig. 2f). To evaluate the degree of synchronism between the oscillators, we exploited the coherence function $|\sigma(f)|$, defined as the averaged cross-spectral density of the oscillations:

$$\sigma(f) = \left\langle \frac{\chi_{x_1}(f)\chi_{x_2}(f)^*}{|\chi_{x_1}(f)||\chi_{x_2}(f)|} \right\rangle, \tag{2}$$

where χ_{x_1} and χ_{x_2} are the spectral densities computed from oscillation $x_1(t)$ or $x_2(t)$, respectively, and f is the frequency.

The magnitude of the coherence function, which will be briefly called the coherence magnitude, characterizes the degree of coherence between the oscillators for each of the spectral components: it is 1 for the frequencies at which the oscillations are coherent and is 0 for those at which the oscillations are totally independent. We define the degree of synchronism between the oscillations as the coherence magnitude averaged over all of the frequencies taking into account the contribution of each spectral component to the total signal power:

$$S = \frac{\int_0^\infty |\sigma(f)|(|\chi_{x_1}(f)|^2 + |\chi_{x_2}(f)|^2)df}{\int_0^\infty |\chi_{x_1}|^2 + |\chi_{x_2}|^2 df}. \tag{3}$$

The degree of synchronism can be viewed as the ratio of the power of synchronous motions in the oscillators to the total oscillation power. It ranges from 0 to 1, the limits respectively corresponding to asynchronous or completely synchronous chaotic oscillations. Note that S is also useful under the conditions other than $\vec{x}_1 = \vec{x}_2$. For example, it works in the case $\vec{x}_1(t) = \vec{x}_2(t - \tau)$, where a synchronous and an asynchronous oscillation

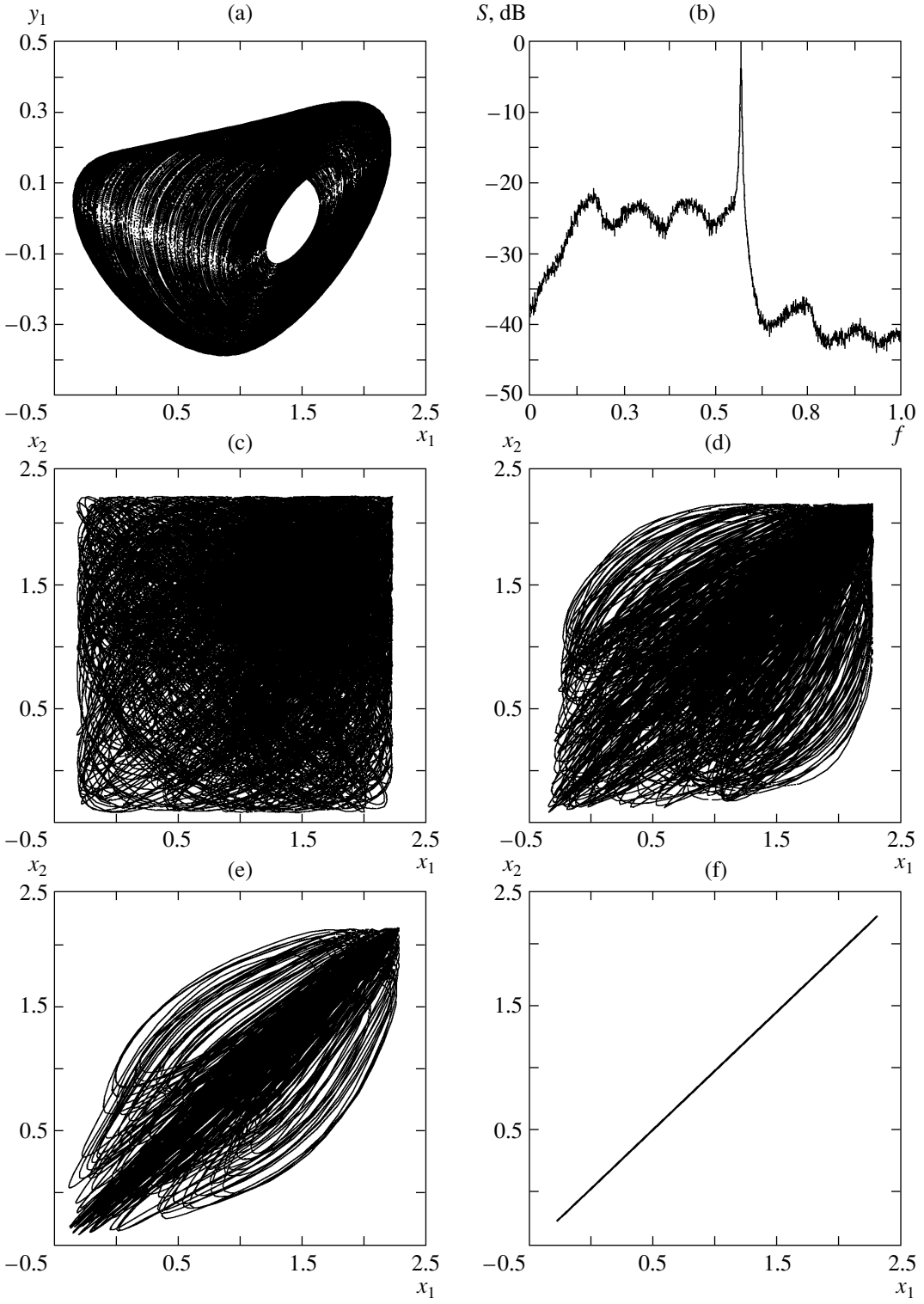

Fig. 2. (a) Projection of the phase portrait onto the x_1–y_1 plane, (b) power spectrum of the chaotic attractor under study, and (c)–(f) the evolution of the projection during the transition from asynchronous to synchronous chaos.

can scarcely be distinguished on the basis of the phase portraits.

Consider the case $p = 1$. Figure 3 shows the evolution of the coherence magnitude, distributed in frequency, with respect to the coupling factor, the degree of synchronism being computed as well. The oscillations in Fig. 3a are nearly asynchronous, the coherence magnitude being close to zero at each frequency. As γ

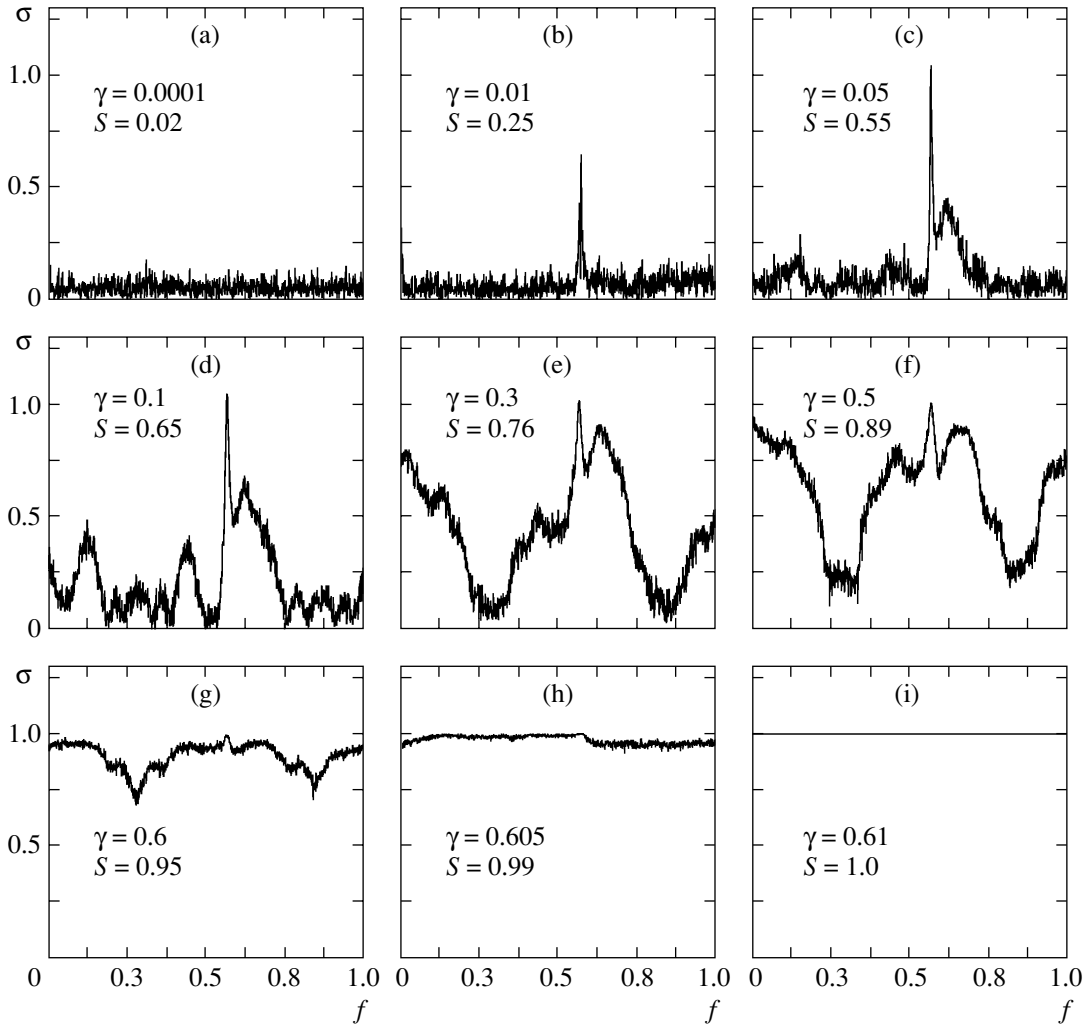

Fig. 3. Coherence magnitude vs. frequency and degree of synchronism, S, for several increasing values of coupling factor γ.

is increased, synchronism develops, first at the frequency f_{max} corresponding to the maximum peak in the spectrum of the attractor (Figs. 3b, 3c) and then in the vicinities of the subharmonic frequencies: $(2k + 1)f_{max}/2$, $(2k + 1)f_{max}/4$, $(2k + 1)f_{max}/8$, and so on (Fig. 3d). Gradually, the degree of synchronism rises, and synchronous portions expand. However, valleys in the plot (Figs. 3e–3i) appear at multiples of $(2k + 1)f_{max}/2$. Finally, at $\gamma = 0.61$, the chaotic oscillations become completely synchronous. Thus, we can conclude that the synchronization in symmetrically coupled and identically adjusted oscillators takes a gradual course, although this seems to involve internal bifurcations related to the restructuring of the attractor phase portrait. It is impossible to definitively draw the line of demarcation between the regions of asynchronous and incompletely synchronous chaos. On the other hand, the boundary between the regions of incomplete and complete synchronism can be delineated in the case $p = 1$ (using the projections of the phase portraits).

Now, look at the case $p \neq 1$. For coupling factor γ, pick a value that would have provided a completely synchronous chaos if p were 1 and that lies near the boundary of the region of synchronism. By contrast, the steady-state oscillations are not synchronous, however small is $p - 1$. (We checked the rule at the values of p down to 1.00001.) The representative point occasionally strays from the symmetric subspace, and the x_1, x_2 projection of the phase portrait becomes smeared (Fig. 4). Figure 5 illustrates the excursions by plotting $\Delta x = x_1 - x_2$ against time. The evolution is essentially marked by on–off intermittence. The magnitude of the bursts is finite at any p and depends only slightly on p. Figure 6 shows the fractional duration of the turbulent phase (Fig. 6a) and the average burst rate (Fig. 6b) as functions of p at different values of γ. The curves first rise steeply, but then they quiet down and run in an almost linear manner. Near $p \sim 1$, the steepness increases as γ approaches the boundary of the region of synchronism, and the functions change abruptly when

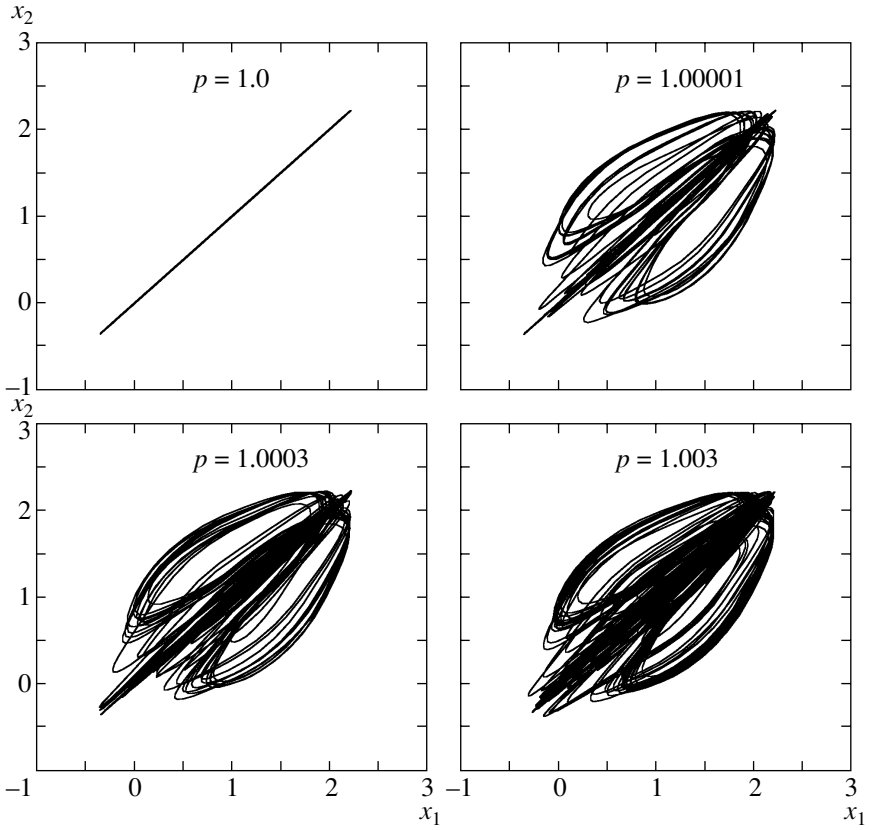

Fig. 4. Projections of phase portraits of chaotic attractors under on–off intermittence.

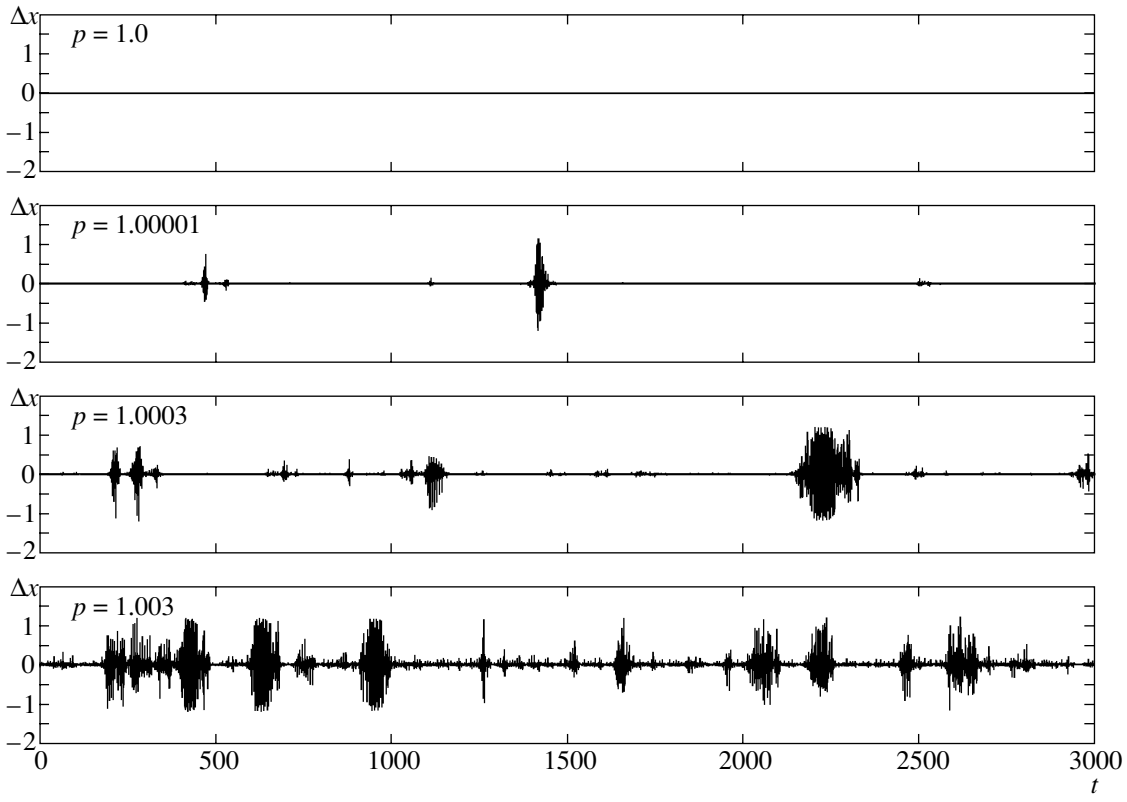

Fig. 5. Time evolution of $\Delta x = x_1 - x_2$ under on–off intermittence.

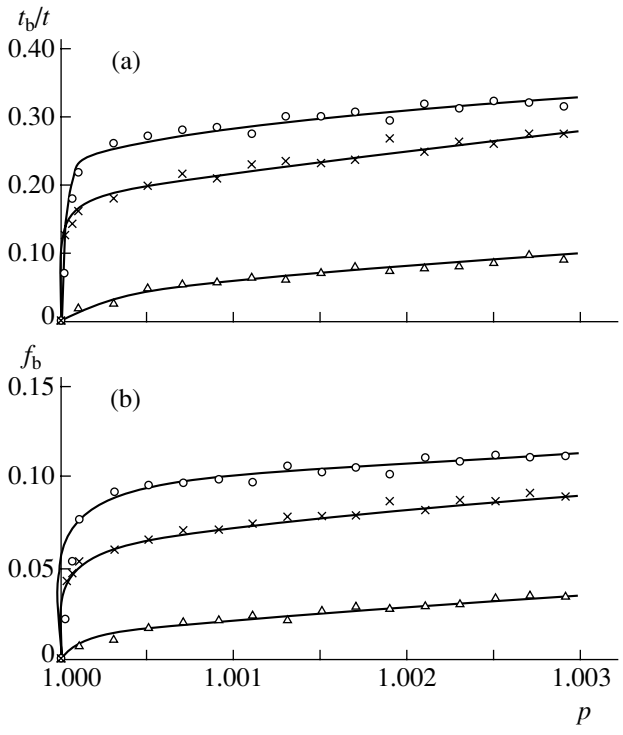

Fig. 6. (a) Fractional duration of the turbulent phase and (b) the average burst rate vs. the mismatch ratio at the coupling factor γ = (△) 0.8, (×) 0.7, and (○) 0.65.

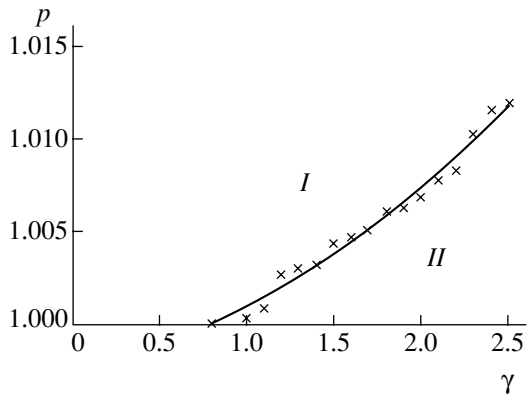

Fig. 7. Threshold mismatch ratio vs. the coupling factor.

the boundary is crossed. With large p, the steepness is independent of γ. Since both the total burst duration and the average burst rate are linear for large p, the duration of the turbulent phase grows by virtue of the increase in the burst rate rather than in the average duration of a burst. Thus, a larger p gives a higher burst rate, but does not affect burst duration.

Figure 6 indicates that on–off intermittence depends on γ. The average number of bursts decreases as γ is increased. An infinitesimal value of $p - 1$ cannot cause the intermittence if $\gamma > 0.8$. This means that synchronism is robust. However, the intermittence arises if p exceeds a certain threshold. Figure 7 shows the threshold value of p plotted against γ. The intermittence is existent in region *I* and nonexistent in region *II*. For the latter region, the attractor corresponding to synchronous oscillations lies in a small neighborhood of the symmetric subspace, the neighborhood contracting as $p \longrightarrow 1$. Thus, with slightly mismatched oscillators, the minimum value of γ that provides a complete synchronism is 0.8 rather than 0.61. Indeed, $\gamma = 0.8$ should be regarded as an actual limit to the region of synchronism: it is this value that is available from physical experiments on system (1).

CONCLUSION

We have studied the chaotic synchronization of coupled oscillators in terms of the coupling factor and the degree of frequency mismatch. Phase portraits and the coherence function were used as indicators of synchronism. It has been found that the transition from asynchronous to completely synchronous chaos proceeds gradually, involving the expansion of the coherent portions of the two oscillation spectra. The frequency approach cannot draw a definite line of demarcation between synchronous and asynchronous chaos. However, phase-portrait projections reveal the bifurcation from an incomplete to a complete synchronism, the latter resulting in the collapse of the attractor to the symmetric subspace $\vec{x}_1 = \vec{x}_2$. If a mismatch is brought in, the coupling factor has been found to determine whether or not complete synchronism is robust. In the region of nonrobust synchronism, on–off intermittence has been observed, the burst rate rising with the mismatch ratio. In the region of robust synchronism, there is a threshold mismatch ratio above which on–off intermittence appears.

ACKNOWLEDGMENTS

This study was supported by the Foundation for Fundamental Sciences, project no. 97-0-8.3-47.

REFERENCES

1. Fujisaka, H. and Yamada, T., *Prog. Theor. Phys.*, 1983, vol. 69, no. 3, p. 32.
2. Afraimovich, V.S., Verichev, N.N., and Rabinovich, M.I., *Izv. Vyssh. Uchebn. Zaved., Radiofiz.*, 1986, vol. 29, no. 9, p. 1050.
3. Abrabanel, H.D.I., Rulkov, N.F., and Sushchik, M.M., *Phys. Rev. E: Stat. Phys., Plasmas, Fluids, Relat. Interdiscip. Top.*, 1996, vol. 53, no. 5, p. 4528.
4. Anishchenko, V.S., Vadivasova, T.E., Postnov, D.E., and Safonova, M.A., *Radiotekh. Elektron.* (Moscow), 1991, vol. 36, no. 2, p. 338.
5. Rosenblum, M.G., Pikovsky, A.S., and Kurths, J., *Phys. Rev. Lett.*, 1996, vol. 76, no. 11, p. 1804.

6. Ashwin, P., Buescu, J., and Stewart, I., *Phys. Lett. A*, 1994, vol. 193, no. 1, p. 126.
7. Ashvin, P., Buescu, J., and Stewart, I., *Nonlinearity*, 1996, vol. 9, p. 703.
8. Hasler, M., Abstracts of Papers, *5th Int. Specialists Workshop on Nonlinear Dynamics of Electronic Systems*, Moscow, 1997, p. 2.
9. Platt, N., Spiegel, E.A., and Tresser, C., *Phys. Rev. Lett.*, 1993, vol. 70, no. 3, p. 279.
10. Anishchenko, V.S., Astakhov, V.V., Vadivasova, T.E., *et al.*, *Int. J. Bifurcation Chaos*, 1995, vol. 5, no. 6, p. 1677.
11. Matsumoto, T., Chua, L.O., and Motomasa, K., *IEEE Trans. Circuits Syst.*, 1986, vol. 32, no. 8, p. 798.
12. Anishchenko, V.S., *Slozhnye kolebaniya v prostykh sistemakh* (Complex Oscillations in Simple Systems), Moscow: Nauka, 1990.
13. Astakhov, V.V., Bezruchko, B.P., Gulyaev, Yu.V., and Seleznev, E.P., *Pis'ma Zh. Tekh. Fiz.*, 1989, vol. 15, no. 3, p. 60.
14. Astakhov, V.V., Shabunin, A.V., Sil'chenko, A.N., *et al.*, *Radiotekh. Elektron.* (Moscow), 1997, vol. 42, no. 3, p. 320.